Coupling heat transfer modelling to ALBA model for full predictions from meteorology

Francesca Casagli, Olivier Bernard

Coupling heat transfer modelling to ALBA model for full predictions from meteorology

Francesca Casagli * **Olivier Bernard** *

* *Université Côte d'Azur, Inria, Biocore, 2004 route des Lucioles, 06902 Sophia-Antipolis Cedex*

Abstract: High Rate Algal-Bacterial Ponds (HRABP) are often considered as an interesting solution for reducing the energy demand due to oxygenation in wastewater treatment, since oxygen is produced by the microalgae during photosynthesis. Modelling these complex dynamical processes is a challenging task since it is subjected to the solar fluxes imposing permanent fluctuations in light and temperature. The ALBA model was developed to represent this process, and validated with 623 days of outdoor measurements, in two different locations and for the four seasons. However, so far this model -as all the other existing models- was not fully predictive since it was requiring the measurement of the water temperature.
The objective of this work is to upgrade the ALgae-BActeria (ALBA) model, coupling it with a physical model predicting the evolution of temperature in the HRABP and presenting a novel structure for the pH submodel implementation. A heat-transfer model was developed and coupled to this model. It was able to accurately (with a standard error of $1.5°C$) predict the temperature along the year. When coupled to the ALBA model, full predictions only based on meteorological data become possible. The predictions are hardly affected compared to using the actual measured temperature, resulting in an overall excellent capability to predict the process behaviour so that it can be further used for the system optimization, and for testing scenarios under very different operating and weather conditions.

Keywords: Microalgae, Bacteria, HRABP, wastewater treatment, heat transfer, temperature

1. INTRODUCTION

The market of the microalgae derived products is in a strong growing phase (Rumin et al., 2020). It includes applications in fish farming, food industry, cosmetics (Koller et al., 2014). Most of the produced biomass is carried out in open raceways (Milledge, 2011). These open ponds agitated by a paddle wheel are cheap production systems, and to date, there is an intense debate to determine whether their actual productivity compared to the closed photobioreactors is significantly lower (Benemann, 2013). Microalgae grown in raceways ponds together with bacteria are also considered as an interesting solution for reducing the energy demand due to oxygenation in wastewater treatment, since oxygen can be brought by the microalgae during photosynthesis.

Productivity in these systems is first driven by the amount of photons which is received by the microalgae, which trigger the photosynthesis reactions. Temperature is the second factor affecting the microalgal growth rate, and it has received much less attention (Ras et al., 2013). Predicting the productivity which can be reached by a raceway at a given location and for a certain period of the year is becoming a key question for upgrading the current wastewater treatment plants including microalgae.

⋆ Sponsor and financial support acknowledgment goes here. Paper titles should be written in uppercase and lowercase letters, not all uppercase.

There are a few modelling studies that represented the dynamics of Algae-Bacteria processes especially for wastewater treatment in High rate Algal-Bacterial Ponds (HRABP) (Reichert et al., 2001; Wolf et al., 2007; Arashiro et al., 2017; Solimeno et al., 2019; Casagli et al., 2021b). Among these models, the ALBA model (Casagli et al., 2021b,a) is probably the most validated with more than 623 days of validation, in outdoor conditions at two different locations and for the four seasons. However, so far all the HRABP models could not be fully predictive since to run they require the knowledge of the water temperature in the medium.

The objective of this work is to propose a new version of the ALBA model, coupling it with a physical model predicting the evolution of the temperature in the HRABP and presenting a novel structure for the pH submodel implementation. The aim was to make the ALBA model fully predictive, so that it can be further used for the system optimization, testing scenarios under very different operating and weather conditions. In fact, temperature is one of the main factor affecting the system performances, especially in outdoor systems, where it is subjected to strong fluctuations both along the day and according to the seasons.

The heat transfer temperature model was implemented on the basis of the work of (Béchet et al., 2011) adapting it to deal with the reactor material and specific configuration. In particular, the dynamics of the temperature for the material of the raceway was added, including the

Fig. 1. Pilot-scale HRABP located close to Milan.

exchange with the liquid medium and the environment. An experimental pilot-scale raceway (1 m^3) located in the north of Italy, in a wastewater treatment plant was considered for the model validation. The fully predictive version of the ALBA model turns out to accurately predict the pond temperature and the variable volume of the raceway, together with the process dynamics, including microalgae, heterotrophic bacteria and nitrifying bacteria.

2. MATERIALS AND METHODS

The HRABP located Milan was a pilot-scale polypropylene tank with an operating volume of 0.88 m^3 and a total surface of approximately 3.8 m^2 (see Figure 1). It was installed in the dedicated treatment plant of an intensive piggery farm, located in the Northern of Italy (Casaletto di Sopra, Cremona, Italy). The influent was made of digestates from the biogas plant. The monitoring campaign was performed from May to December 2016. The HRABP influent was prepared from the liquid fraction of the digestate, and by dilution with tap water in order to reduce the influent TAN (Total Ammoniacal Nitrogen) concentration. The open pond mixing was ensured by a paddle wheel, that was operated at 20 rpm to obtain an average liquid velocity of 0.2 m s^{-1}. The reactor was also equipped with a contact cylinder (height 0.8 m, diameter 0.44 m, volume 0.12 m^3) for bubbling pure CO_2 gas to regulate pH. An average Hydraulic Retention Time (HRT) of 10 days was set until 11/10/2016, then the HRT was increased to 20 days, in order to compensate for the temperature reduction occurring with the incoming cold season. The outflow was from a gravity overflow, resulting in a variable volume according to evaporation and rain contribution (A.Pizzera et al., 2019). The meteorological data were provided by ARPA Lombardia regional meteo database. The environmental conditions at the reactor location (i.e. air temperature, relative humidity, wind speed and rain rate), were provided by ARPA Lombardia regional meteo database.

3. MODELLING APPROACH

3.1 The ALBA model: brief recall of the core structure

The biological ALBA model considers a mixed culture of algae (X_{ALG}), heterotrophic bacteria (X_H), Ammonium Oxidizing Bacteria (X_{AOB}) and Nitrite Oxidizing Bacteria (X_{NOB}). The nomenclature are in line with the IWA modelling works, i.e. Activated Sludge Models (ASMs) and Anaerobic Digestion Model n°1 (ADM1) (Batstone et al., 2001; Henze et al., 2000).

The model includes 19 biological processes and involves 17 state variables. The general model structure follows the general mass balance structure (Bastin and Dochain (1990)):

$$\dot{\xi} = K \cdot \rho(\xi) - \Delta_g(\xi) + \frac{Q_{in}}{V} \cdot \xi_{in} - \frac{Q_{out}}{V} \cdot \xi \qquad (1)$$

where $Q_{out} = Q_{in} + Q_{rain} - Q_{evap}$. ξ is the state variable vector $[gm^{-3}]$; ξ_{in} is the vector of influent concentrations [g m^{-3}];$\rho(\xi)$ is the vector containing the reaction rates $[gm^{-3}d^{-1}]$; Q_{in}, Q_{rain} and Q_{evap} are the inflow rate, rain rate and evaporation rate, respectively $[m^3d^{-1}]$; K is the stoichiometric matrix (the transpose of the Petersen matrix); V is the liquid volume $[m^3]$. The flux of gases dissolving or stripping from the liquid medium is denoted $\Delta_g(\xi)$ $[gm^{-3}d^{-1}]$.

The biokinetic rates are based on the Liebig's minimum law (De Baar, 1994) for limiting substrates (carbon, nitrogen and phosphorus), meaning that the most limiting nutrient drives the overall kinetics. The general expression describing the structure of the bioprocesses rates is given by:

$$\rho_j = \mu_{max_j} \cdot f_T \cdot f_{pH} \cdot f_I \cdot \frac{K_n}{K_n + S_n} \cdot \min_i \left(\frac{S_i}{S_i + K_{S_i}} \right) \cdot X_{BM_i} \qquad (2)$$

Where: μ_{max_j} is the maximum specific growth rate [d^{-1}] related to the process ρ_j; f_T, f_{pH} and f_I are the functions describing temperature, pH and light dependence, respectively; K_n is the inhibition constant for the inhibiting substrate S_n, K_{S_i} is the half-saturation constant for the limiting substrate S_i and $X_{BM,i}$ is the biomass associated to the process ρ_j.

Light is a crucial factor for algal growth, driving a large fraction of the energy and carbon fluxes in the system. Light extinction is described by the Lambert-Beer equation:

$$I(I_0, z) = I_0 e^{-\epsilon X_{ALG} z} \qquad (3)$$

where $I(I_0, z)$ is the PAR (Photosynthetically Active Radiation) value $[molm^{-2}s^{-1}]$ measured at the depth z $[m]$; $I(0)$ is the PAR value $[molm^{-2}s^{-1}]$ measured at the reactor surface z=0 m; X_{ALG} is the algae concentration of the algal suspension $[gm^{-3}]$ and ϵ is the light extinction coefficient $[m^2g^{-1}]$. The photosynthesis response to irradiance at depth z accounts for the photoinhibition phenomena at high irradiance with the Haldane-type function (Bernard and Rémond, 2012):

$$f_{opt}(I(z)) = \frac{I(z)}{I(z) + \frac{\mu_{max}}{\alpha} \left(\frac{I(z)}{I_{opt}} - 1 \right)^2} \qquad (4)$$

Finally, the average growth rate for a given incident light and liquid depth is obtained, integrating the growth rate along depth:

$$f_I(I_0, h) = \frac{1}{h} \int_0^h f_{opt}(I(I_0, z)) dz \qquad (5)$$

The temperature in HRABP (T_p) is typically not controlled, so that it fluctuates within large ranges according to daily and seasonal dynamics. The prediction of temperature fluctuation will be the subject of the next paragraph.

The temperature dependence for algae and bacteria growth is modelled through the Cardinal Temperature Model with Inflection (CTMI), that requires three parameters, i.e. the cardinal temperatures: T_{max}, T_{min} and T_{opt}, (Rosso et al., 1995). The CTMI is zero for $T_p \notin [T_{min},\ T_{max}]$, where T_{min} is the temperature below which no growth occurs and T_{max} is the maximum temperatures above which no growth occurs. T_{opt} is the temperature at which the growth rate is maximum. For $T_p \in [T_{min},\ T_{max}]$ the temperature effect is given by the function $f_{T_p,1}$:

$$f_{T_p,1} = \frac{(T_p - T_{max}) \cdot (T_p - T_{min})^2}{(T_{opt} - T_{min}) \cdot \Phi(T_p)} \tag{6}$$

where $\Phi(T_p) = (T_{opt} - T_{min}) \cdot (T_p - T_{opt}) - (T_{opt} - T_{max}) \cdot (T_{opt} + T_{min} - 2T_p)$

The Arrhenius function was chosen for the decay rates:

$$f_{T,2} = \theta^{T_p - 20} \tag{7}$$

where the parameter θ provides the decay rate.

The pH strongly influences system dynamics, since it directly affects the dissociation of the majority of soluble compounds (S_{IC}, S_{NH}, S_{NO2}, S_{NO3}, S_{PO4}). The influence of pH on algae and bacteria bio-process rates is included through the function proposed by Rosso et al. (1995), i.e. the Cardinal pH Model (CPM). The CPM is zero for $pH \notin [pH_{min},\ pH_{max}]$, where pH_{min} and pH_{max} are the minimum and the maximum pH thresholds respectively. pH_{opt} is the pH value at which the growth rate is maximum. For $pH \in [pH_{min},\ pH_{max}]$ the pH effect is described by f_{pH}:

$$f_{pH} = \frac{(pH - pH_{max}) \cdot (pH - pH_{min})}{(pH - pH_{min}) \cdot (pH - pH_{max}) - (pH - pH_{opt})^2} \tag{8}$$

The pH is estimated by the model, resulting from the dynamical balance between the chemical, physical and biological process interactions. The pH sub-model is based on dissociation equilibria and mass balances of acids and bases, according to the one proposed in the ADM1 and on the charge balance, through which the concentration of hydrogen ions is computed.

The CO_2, O_2 stripping/dissolution and NH_3 stripping are also included, quantifying their rates through the k_La and their diffusion coefficients:

$$Q_j = k_L a_j \cdot \left(\frac{D_{S_j}}{D_{S_{O2}}}\right)^2 \cdot (S_{j,sat}(T_p) - S_j) \tag{9}$$

A more detailed description of the ALBA model can be found in (Casagli et al., 2021b), together with i) the model prediction capability for the monitored variables of another experimental case study with a 68 m^2 located in France, with long term monitoring of pH, S_{O2}, S_{NH}, S_{NO3}, S_{NO2}, X_{ALG}, TSS and soluble COD, ii) the sensitivity analysis, calibration and validation procedure, iii) the analysis of carbon and nitrogen fluxes under period regime and according to seasonal variability.

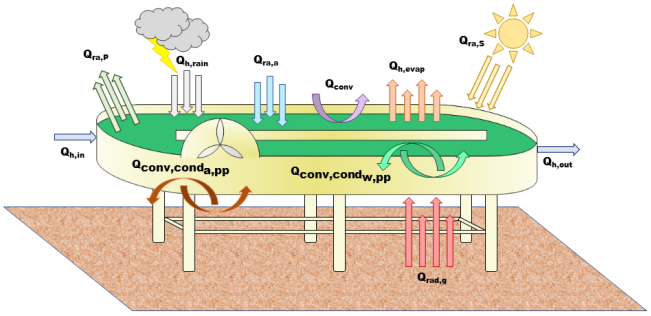

Fig. 2. Heat fluxes considered in the radiative transfer model.

3.2 Predicting pond temperature and water level

The universal temperature model for shallow ponds developed by Béchet et al. (2011) was adapted to predict the water temperature and the water level of the raceway. The existing radiative transfer model was modified, to deal with the fact that this raceway was suspended above the ground. Other heat fluxes had to be considered (see Figure 2), and a heat balance of the raceway material was also considered.

The model simulates the temperature changes in the algal pond according to the heat balance:

$$\begin{aligned} \rho_w V C_{p,w} \frac{dT_p}{dt} &= Q_{ra,p} + Q_{ra,s} + Q_{ra,a} + \\ &+ Q_{h,evap} + Q_{conv} + Q_{h,in} + \\ &+ Q_{h,out} + Q_{h,rain} - Q_{conv,cond_w,pp} \end{aligned} \tag{10}$$

where T_p is the pond temperature [K]; ρ_w is the density of pond water [kg m^{-3}]; $C_{p,w}$ is the specific heat capacity of the pond water [J kg^{-1} K^{-1}]; and V is the pond volume [m^3]. $Q_{ra,p}$ is the radiation from the pond surface [W]; $Q_{ra,s}$ is the total (direct + diffuse) solar radiation [W]; and $Q_{ra,a}$ is the radiation from the air of the pond [W]. $Q_{h,evap}$ is the evaporation flux (W), Q_{conv} is the convective flux at the pond surface [W]; $Q_{h,in}$ is the heat flux associated with the influent water [W];$Q_{h,out}$ is the heat flux associated to the effluent water [W]; $Q_{h,rain}$ is the heat flux related to rain [W].
The two additional terms $Q_{conv,cond_w,pp}$ and $Q_{conv,cond_a,pp}$ are the conductive/convective expressions related to the heat exchange between the water in the pond and the material of the HRABP at the bottom (here polypropylene (pp)):

$$Q_{conv,cond_w,pp} = h_{w,pp} \cdot (T_p - T_{pp})S \tag{11}$$

and the air and the raceway at the bottom part:

$$Q_{conv,cond_a,pp} = h_{a,pp} \cdot (T_a - T_{pp})S \tag{12}$$

The parameter $h_{w,pp}$ [W m^{-2} K^{-1}] is the heat transfer coefficient between the water in the pond (w) and the polypropylene, T_{pp} [K] is the temperature of the polypropylene; the parameter $h_{a,pp}$ [W m^{-2} K^{-1}] is the heat transfer coefficient between the air (a) and the polypropylene and T_a [K] is the air temperature.

The HRABP was raised from the ground, as shown in figure 1. A heat balance on the material of the pond is therefore also carried out:

$$\rho_{pp}V_{pp}C_{p,pp}\frac{dT_{pp}}{dt} = Q_{conv,cond_w,pp} + Q_{conv,cond_a,pp} + Q_{ra,pp} + Q_{ra,a,pp} + Q_{rad,d} \quad (13)$$

Where $Q_{ra,pp}$ is the pond radiation at the bottom of the reactor:

$$Q_{ra,pp} = -\epsilon_{pp} \cdot \sigma \cdot T_{pp}^4 \cdot S \quad (14)$$

and $Q_{ra,a,pp}$ is the expression describing the air radiation at the bottom of the pond, on the polypropylene surface:

$$Q_{ra,a,pp} = \epsilon_{pp} \cdot \epsilon_a \cdot \sigma \cdot T_a^4 \cdot S \quad (15)$$

Finally, $Q_{rad,g}$ is the radiation from the ground to the pond bottom:

$$Q_{rad,g} = -\epsilon_{ground} \cdot \sigma \cdot T_g^4 \cdot S \quad (16)$$

The temperature of the ground was computed from the air temperature, following Tsilingiridis and Papakostas (2014):

$$T_g = 1.197 \cdot T_a - 0.7776; \quad (17)$$

The parameters ϵ_{ground}, ϵ_{pp} and ϵ_a are the emissivity of the ground, polypropylene and air respectively [-]; σ is the Stephan-Boltzmann constant $[Wm^{-2}K^{-4}]$.

The evaporative and convective heat flux in the liquid medium have a marked effect on the pond temperature prediction, and they were implemented according to the Buckinngham theorem, depending on the dimensionless numbers of Sherwood, Schmidt and Reynolds. The Sherwood and Nusselt numbers were linearly interpolated for Reynolds numbers between 3×10^5 and 5×10^5 to ensure model calculations for Reynolds numbers in the transition from laminar to turbulent flow. For the calculation of the evaporative heat flux, a minimum wind speed (4 m s^{-1}) was considered, as the equation for evaporative heat flux does not account for evaporation when there is no wind.

From the evaporation and rain heat fluxes, it is possible to evaluate the water level variation in the pond:

$$S\frac{dh_L}{dt} = \frac{-m_e}{\rho_w} + Q_{rain} + Q_{in} - Q_{out} \quad (18)$$

where m_e is the evaporation rate $[Kgs^{-1}m^{-2}]$; ρ_w is the water density $[Kgm^{-3}]$; Q_{rain} is the rain rate $[m^3s^{-1}]$; Q_{in} is the inflow rate $[m^3s^{-1}]$.

3.3 Chemical sub-model implementation

The chemical submodel consists in predicting pH ($[H^+]$ ions concentration), but also computing the fraction of the different dissociated compounds which are in equilibrium depending on the pH. This sub-module includes three ingredients:

(1) The mass balance equations for the state variables corresponding to the total sum of chemicals which dissociate in the water. As an example, the total concentration of NH_3 and NH_4^+ in the model corresponding to the state variable $\frac{S_{NH}}{14}$ leads to the following mass balance equation:

$$\frac{S_{NH}}{14} - NH_3 - NH_4^+ = 0$$

Note that these equations also account for the change in unit between the state variables and the chemical model (which should be in mol.m^{-3}).

(2) The dissociation equations representing the affinity constants. They must be rewritten in a form where only the H^+ ions concentration together with the total amount of the element appears (represented by one of the model state variable). For example, for the dissociation constant associated with the chemical equilibrium $NH_4^+ \rightleftharpoons NH_3 + H^+$:

$$NH_4^+ = \frac{S_{NH}/14}{1 + \frac{Ka_{NH_4}10^3}{H^+}}$$

(3) The ionic balance equation representing the electroneutrality of the medium, accounting for all the ions that are affected by the reactions, and for those of constant concentration (denoted $\Delta_{CAT,AN}$) whose concentrations are not modified by any biochemical reaction. The considered electroneutrality equation is:

$$H^+ + NH_4^+ = OH^- + NO_2^- + NO_3^- + HCO_3^- + 2CO_3^{2-} + H_2PO_4^- + 2HPO_4^{2-} + 3PO_4^{3-} - \Delta_{CAT,AN} \quad (19)$$

The temperature influence on the acidity constants was taken into account by using the van't Hoff equation:

$$ln\frac{K_{a,T_p}}{K_{a,T_{ref}}} = \frac{\Delta H}{R}\left(\frac{1}{T_{ref}} - \frac{1}{T_p + 273.15}\right) \quad (20)$$

where T_{ref} is the standard temperature (i.e. 298.15 K) for which the value of the equilibrium coefficient ($K_{a,T_{ref}}$, $[molL^{-1}]$) is known, K_{a,T_p}, $[molL^{-1}]$ is the equilibrium coefficient at T_p, R is the gas law constant $[JK^1mol^1]$ and ΔH is the heat of reaction at standard temperature and pressure $[Jmol^{-1}]$.

The strategy for resolving the pH subsystem was inspired by Rosén and Jeppsson (2006). The idea was to transform the initial problem of resolution of a set of algebraic equations resulting from mass balance and affinity constant into the solution of a differential system. It consists in determining 15 unknown (NH_3, NH_4^+, NO_2^-, HNO_2, NO_3^-, HNO_3, CO_2, HCO_3^-, CO_3^{2-}, $H_3PO_4, H_2PO_4^-$, HPO_4^{2-}, PO_4^{3-}, OH^- and H^+) from the 5 state variables $S_{PO_4}, S_{NO_2}, S_{NO_3}, S_{NH}$ and S_{IC} supporting the 5 mass balances and the 9 equations for the dissociation. In the end, the charge balance provides the equation in which only the unknown $[H^+]$ will appear. Equation (19) can be rewritten accounting for the dependence of the dissociated fractions from the H^+ ions and from the total amount of compounds.

$$\begin{aligned} H^+ \; & +NH_4^+(H^+, S_{NH}) + \Delta_{CAT,AN} - OH^-(H^+) \\ & -NO_2^-(H^+, S_{NO_2}) - NO_3^-(H^+, S_{NO_3}) \\ & -HCO_3^-(H^+, S_{IC}) \\ & -2CO_3^{2-}(H^+, S_{IC}) - H_2PO_4^-(H^+, S_{PO_4}) \\ & -2HPO_4^{2-}(H^+, S_{PO_4}) - 3PO_4^{3-}(H^+, S_{PO_4}) \; = 0 \end{aligned} \quad (21)$$

which can be summarised as

$$H^+ = \Phi_{\mathrm{pH}}(H^+, S_{PO_4}, S_{NO_2}, S_{NO_3}, S_{NH}, S_{IC}) \quad (22)$$

The physical root of this equation can be solved by an algebraic solver. Here we prefer to compute the variable $\hat{H}^+$ which is an estimate of H^+. The estimator equation is given by

$$\frac{d\hat{H}^+}{dt} = \hat{K}\left(\Phi_{\mathrm{pH}}(\hat{H}^+, S_{PO_4}, S_{NO_2}, S_{NO_3}, S_{NH}, S_{IC}) - \hat{H}^+\right)$$

where $\hat{K}$ is a constant tuning the rate for solving the pH equation. Note that, once at equilibrium, $\hat{H}^+$ automatically satisfies Equation (22).

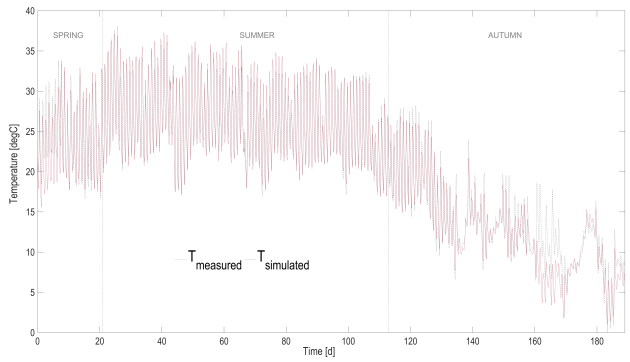

Fig. 3. Temperature predictions (red continuous line) vs measurements (grey dotted line) in the HRABP

4. RESULTS AND DISCUSSION

4.1 Validating the temperature model

The temperature predictions are accurate, as it can be seen in figure 3 and in Table 1. The model tends to slightly overestimate the temperature in the hotter periods and to underestimate it in the cooler periods. The temperature predictions remain anyway accurate, with a standard deviation of $1.6°C$.

State variable	Err.St.Dev. (av)	Abs.Rel.Err. (av %)	Coeff.Var. (-)	R^2 (-)
S_{NH}	0.9165	3.0531	0.0170	0.9994
S_{NO2}	1.7102	7.7069	0.1004	0.9982
S_{NO3}	1.8548	1.6769	0.0087	0.9997
X_{ALG}	14.6689	2.5129	0.0291	0.9940
TSS	10.3061	1.7773	0.0228	0.9952
$CODs$	0.6988	0.3022	0.0023	0.9998
S_{O2}	0.4511	2.8032	0.0533	0.9844
pH	0.0531	0.4669	0.0080	0.9912
T^*	1.6178	7.4652	0.0774	0.9628

Table 1. Comparison between simulated variables using temperature measurements and predictions from the fully predictive model. (*): for temperature, the comparison is between the measured and the simulated one.

Model predictions could be further improved by tuning some of the model parameters, or by using a dedicated meteorological station providing a more accurate estimation of the environmental conditions at the pond location. In fact, the weather dataset used for running simulations were coming from the meteorological station located at a distance of 10 Km from where the reactor.

4.2 Full predictive ALBA model

In order to evaluate the overall model prediction capability using the predicted temperature, instead of the one measured with the probe, dynamic simulations were then run. The most relevant model state variables are reported in Figures 4 and 5, and compared with the experimental measurements, their standard deviations and the error bounds for model predictions.

The accuracy of the heat transfer model results in predictions which are almost unchanged compared to the ones using the measured temperature (see Table

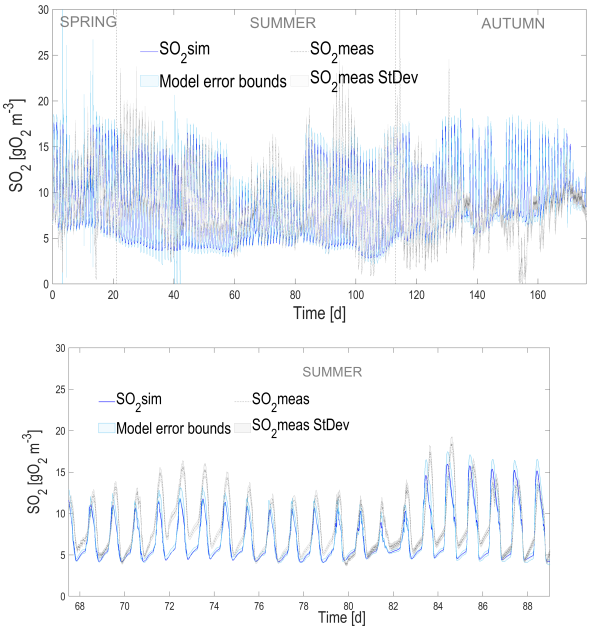

Fig. 4. Full prediction capability of the coupled thermal-biological ALBA model compared with the measurements for dissolved oxygen (SO_2). In the lower figure there is a zoom on summer season. Blue shaded areas are the model error bounds, while grey shaded areas represent the standard deviations for the measured data.

1). When comparing the predicted measurements of the initial model with measured temperature and the new one with predicted temperature, the r^2 is always larger than 0.98 for 2000 simulated points and the predicted variables stay within an interval of 3% compared to the values simulated using the measured temperature.

5. CONCLUSIONS

This work presents the ALBA model coupled with the heat transfer module. This is probably the first fully predictive model for simulating outdoor Algae-Bacteria process efficiency from meteorological databases, or even from the weather forecasts. The model predictions stay very accurate so that it can be further used for process optimization, and for testing scenarios under different operating strategies, opening the door to Model Predictive Control for improving the management of this complex process.

ACKNOWLEDGEMENTS

The authors acknowledge the support of the ADEME Biomsa project.

REFERENCES

A.Pizzera, Scaglione, D., Bellucci, M., Marazzi, F., Mezzanotte, V., Parati, K., and Ficara, E. (2019). Digestate treatment with algae-bacteria consortia: A field pilot-scale experimentation in a sub-optimal climate area. *Bioresource Technology*, 274, 232–243.

Arashiro, L.T., Rada-Ariza, A.M., Wang, M., Van Der Steen, P., and Ergas, S.J. (2017). Modelling shortcut nitrogen removal from wastewater using

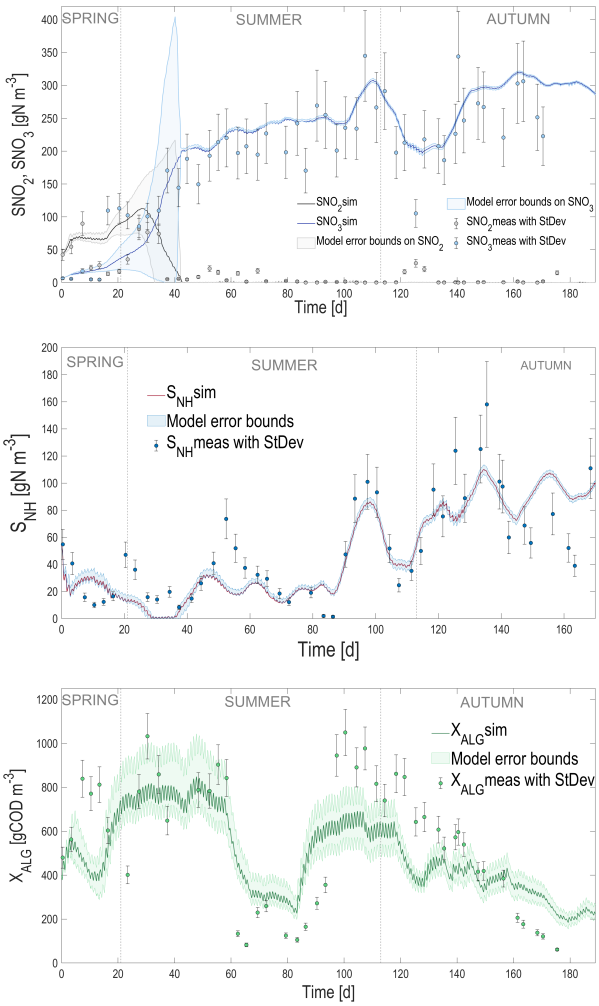

Fig. 5. Full prediction capability of the coupled thermal-biological ALBA model. Comparison between full predictions (with simulated temperature) and measurements for ammoniacal nitrigen (S_{NH}), nitrite (S_{NO_2}), nitrate (S_{NO_3}) and algal biomass (X_{ALG}). Shaded areas represent the model error bounds.

an algal–bacterial consortium. *Water Science and Technology*, 75(4), 782–792.

Bastin, G. and Dochain, D. (1990). *On-line estimation and adaptive control of bioreactors*. Elsevier, New York.

Batstone, D., Keller, J., Angelidaki, R.I., Kalyuzhnyi, S.V., Pavlostathis, S.G., Rozzi, A., Siegrist, W.T.M.S.H., and Vavilin, V.A. (2001). The IWA anaerobic model no 1 . In *Proceedings of the 9th IWA World Congress on Anaerobic digestion*. Antwerp, Belgium.

Béchet, Q., Shilton, A., Park, J.B., Craggs, R.J., and Guieysse, B. (2011). Universal temperature model for shallow algal ponds provides improved accuracy. *Environmental science & technology*, 45(8), 3702–3709.

Benemann, J. (2013). Microalgae for biofuels and animal feeds. *Energies*, 6(11), 5869–5886.

Bernard, O. and Rémond, B. (2012). Validation of a simple model accounting for light and temperature effect on microalgal growth. *Bioresource technology*, 123, 520–527.

Casagli, F., Rossi, S., Steyer, J.P., Bernard, O., and Ficara, E. (2021a). Balancing microalgae and nitrifiers for wastewater treatment: can inorganic carbon limitation cause an environmental threat? *Environmental science & technology*, 55(6), 3940–3955.

Casagli, F., Zuccaro, G., Bernard, O., Steyer, J.P., and Ficara, E. (2021b). Alba: A comprehensive growth model to optimize algae-bacteria wastewater treatment in raceway ponds. *Water Research*, 190, 116734.

De Baar, H. (1994). von liebig's law of the minimum and plankton ecology (1899–1991). *Progress in oceanography*, 33(4), 347–386.

Henze, M., Gujer, W., Mino, T., and Van Loosdrecht, M. (2000). *Activated sludge models ASM1, ASM2, ASM2d and ASM3*. IWA publishing.

Koller, M., Muhr, A., and Braunegg, G. (2014). Microalgae as versatile cellular factories for valued products. *Algal research*, 6, 52–63.

Milledge, J.J. (2011). Commercial application of microalgae other than as biofuels: a brief review. *Reviews in Environmental Science and Bio/Technology*, 10(1), 31–41.

Ras, M., Steyer, J.P., and Bernard, O. (2013). Temperature effect on microalgae: a crucial factor for outdoor production. *Reviews in Environmental Science and Bio/Technology*, 12(2), 153–164.

Reichert, P., Borchardt, D., Henze, M., Rauch, W., Shanahan, P., Somlyódy, L., and Vanrolleghem, P. (2001). River water quality model no. 1 (rwqm1): Ii. biochemical process equations. *Water Science and Technology*, 43(5), 11–30.

Rosén, C. and Jeppsson, U. (2006). Aspects on ADM1 Implementation within the BSM2 Framework. *Department of Industrial Electrical Engineering and Automation, Lund University, Lund, Sweden*.

Rosso, L., Lobry, J., Bajard, S., and Flandrois, J.P. (1995). Convenient model to describe the combined effects of temperature and ph on microbial growth. *Applied and environmental microbiology*, 61(2), 610–616.

Rumin, J., Nicolau, E., Gonçalves de Oliveira Junior, R., Fuentes-Grünewald, C., and Picot, L. (2020). Analysis of scientific research driving microalgae market opportunities in europe. *Marine drugs*, 18(5), 264.

Solimeno, A., Gómez-Serrano, C., and Acién, F.G. (2019). Bio_algae 2: improved model of microalgae and bacteria consortia for wastewater treatment. *Environmental Science and Pollution Research*, 26(25), 25855–25868.

Tsilingiridis, G. and Papakostas, K. (2014). Investigating the relationship between air and ground temperature variations in shallow depths in northern greece. *Energy*, 73, 1007–1016.

Wolf, G., Picioreanu, C., and van Loosdrecht, M.C. (2007). Kinetic modeling of phototrophic biofilms: the phobia model. *Biotechnology and bioengineering*, 97(5), 1064–1079.